Pharmacologic Suppression of Inflammation by a Diphenyldifluoroketone, EF24, in a Rat Model of Fixed-Volume Hemorrhage Improves Survival

Vivek R. Yadav, Kaustuv Sahoo, Pamela R. Roberts, and Vibhudutta Awasthi

Department of Pharmaceutical Sciences (V.R.Y., K.S., V.A.) and Department of Anesthesiology (P.R.R.), University of Oklahoma Health Science Center, Oklahoma City, Oklahoma

ABSTRACT

An exaggerated release of proinflammatory cytokines and accompanying inflammation contributes to the development of multiple organ failure after hemorrhagic shock. Here, we tested the nuclear factor (NF) κ-light-chain-enhancer of activated B cell (NF-κB)–mediated transcriptional control of inflammatory pathways as a target in the management of hemorrhage-induced inflammation. We performed a study in a rat model of fixed-volume hemorrhage to investigate the anti-inflammatory effects of the diphenyldifluoroketone EF24 [3,5-bis(2-fluorobenzylidene) piperidin-4-one], an NF-κB inhibitor, in lung tissue. EF24 treatment (0.4 mg/kg) significantly prevented the upregulation of inflammatory biomarkers in rats subjected to 50% hemorrhage and preserved the pulmonary histology in hemorrhaged rats. The lung tissue from treated rats showed marked suppression of the hemorrhage-mediated induction of Toll-like receptor 4, phospho-p65 NF-κB, inducible nitric-oxide synthase, heme oxygenase–1, and cyclooxygenase-2 (COX-2). The hemorrhage-induced COX-2 activity was also significantly inhibited by the EF24 treatment. At the same time, EF24 induced nuclear factor (erythroid-derived 2)-like 2–mediated protective mechanisms against oxidative stress. EF24 also reduced hemorrhage-induced lung myeloperoxidase activity. The plasma levels of proinflammatory tumor necrosis factor-α, interleukin (IL)-6, IL-1α, and IL-1β were lower in EF24-treated rats than in untreated rats. Moreover, there was a significant reduction in the pulmonary expression of high-mobility group B1 protein. These biochemical effects were accompanied by a significant improvement in the survival of rats administered with EF24 as compared with the rats receiving vehicle control ($P < 0.05$). Overall, the results suggest that EF24 attenuates hemorrhage-induced inflammation and could serve as a salutary anti-inflammatory agent in resuscitation strategies.

Introduction

Tissue inflammation triggered by hemorrhage and aggravated by reperfusion often results in irreversible organ damage. The mortality and morbidity associated with hemorrhagic shock (HS) is described as multiple organ dysfunction syndrome. The pathophysiology of multiple organ dysfunction syndrome is complex, but in part is attributed to the excessive activation of inflammatory pathways following traumatic injury (Peitzman et al., 1995; Bone, 1996; Namas et al., 2009; Mi et al., 2011). Normally, the inflammatory response is self-limiting, and its initiation and resolution are orchestrated by a complex interplay among the instructive cytokines and immune cells (Fukunaga et al., 2005; Karin et al., 2006). Because of the severity and acute nature of ischemic injury in HS, the innate arm of the immune system exercises the initial control. Much of the innate response depends on the expression of pattern recognition receptors (PRRs) associated with the antigen-presenting cells. Unlike the adaptive arm of the immune system, the PRRs enable a rapid control of tissue insult and homeostasis (Mollen et al., 2006). For instance, Toll-like receptor 4 (TLR4) is a PRR that specializes in the recognition and concomitant signaling of highly conserved damage-associated molecular patterns (DAMPs) or pathogen-associated molecular patterns. Because of their early participation after hemorrhage, TLR4 and related pathways are potential targets for swiftly controlling the inflammatory response. Left unmanaged, the inflammatory response becomes a self-perpetuating process resulting in widespread and irreversible organ dysfunction.

The signaling networks from various PRRs converge on the transcription element nuclear factor (NF)-κB, which orchestrates the inflammatory response through effector cytokines, such as tumor necrosis factor (TNF)-α and interleukin (IL)-6,

ABBREVIATIONS: APE1, apurinic endonuclease; COX-2, cyclooxygenase-2; DAMP, damage-associated molecular pattern; EF24, 3,5-bis(2-fluorobenzylidene)piperidin-4-one; ELISA, enzyme-linked immunosorbent assay; EP, ethyl pyruvate; HEM, hemorrhage; HMGB1, high-mobility group box 1; HO-1, heme oxygenase–1; HRP, horseradish peroxidase; HS, hemorrhagic shock; HTAB, hexadecyltrimethylammonium bromide; IFN-γ, interferon-γ; IL, interleukin; iNOS, inducible nitric-oxide synthase; I/R, ischemia/reperfusion; MAP, mean arterial blood pressure; MCP-1, monocyte chemotactic protein–1; MIP, macrophage inflammatory protein; NF-κB, nuclear factor-κB; OGG1, 8-oxoguanine DNA glycosylase 1; PRR, pattern recognition receptor; RANTES, regulated and normal T-cell expressed and secreted; SOD1, superoxide dismutase 1; TLR4, Toll-like receptor 4; TNF, tumor necrosis factor.

as well as by the transcriptional control of the inflammatory pathway (Newton and Dixit, 2012). A critical step in the pathway leading up to the synthesis of inflammatory eicosanoids is catalyzed by cyclooxygenase-2 (COX-2). NF-κB also functions upstream of *COX-2* gene to control its transcription (Tsatsanis et al., 2006). These advances in the molecular understanding of TLR4/NF-κB signaling provide a sound basis for a hypothesis that modulation of NF-κB could be beneficial in mitigating the inflammation in HS (Wu, 2006). However, studies directly targeting NF-κB in hemorrhage-associated inflammation are lacking.

Recently, we reported that a novel compound, EF24 (3,5-bis [2-fluorobenzylidene]piperidin-4-one), potently suppresses NF-κB activation, modulates dendritic cell phenotype, and reduces secretion of proinflammatory cytokines TNF-α and IL-6 (Vilekar et al., 2012). The putative mechanism of its action is based on its ability to suppress NF-κB activation by inhibiting the catalytic activity of IκB kinase (Kasinski et al., 2008). EF24 belongs to the *chalcone* group of chemicals and exhibits antiproliferative activity against cancer cells, both in vitro and in vivo (Subramaniam et al., 2008; Lagisetty et al., 2010). Herein, we report for the first time the systemic anti-inflammatory effects of EF24 in a rat model of fixed-volume hemorrhage. Even in the absence of resuscitation for correction of oxygen or volume deficit, the administration of a small volume of aqueous solution of EF24 significantly prolonged the survival of rats subjected to hemorrhage.

Materials and Methods

EF24 was synthesized in-house by the procedure published elsewhere (Lagisetty et al., 2010). For all the experiments, a sterile solution of EF24 was prepared in water having endotoxin content less than 0.1 EU/ml (Caisson Laboratories, North Logan, UT). The primary rabbit antibodies against rat antigens were obtained from Cell Signaling Technology (Danvers, MA), Santa Cruz Biotechnology (Santa Cruz, CA), Abcam (Cambridge, MA), Epitomics (Burlingame, CA), and Sigma-Aldrich (St. Louis, MO). Horseradish peroxidase (HRP)-conjugated secondary goat anti-rabbit IgG and rabbit anti-goat IgG antibodies were from either Cell Signaling Technology (No. 7044) or Sigma-Aldrich (A5420). All other chemicals were obtained from various vendors represented by VWR International (Radnor, PA).

Rat Model of Fixed-Volume Hemorrhage. The animal experiments were performed according to the National Institutes of Health Animal Use and Care Guidelines and were approved by the Institutional Animal Care Committee of the University of Oklahoma Health Sciences Center. The rat hypovolemic model has been described elsewhere (Awasthi et al., 2007). In brief, the left femoral artery of male Sprague-Dawley rats (250–300 g) was cannulated with a catheter consisting of Tygon tubing (0.02 × 0.06 inches) coupled to a 2.5-inch polytetrafluoroethylene tip (28 gauge). Hemorrhagic experiments were performed after allowing 2 days of recovery. The cannulated rats were randomized in three groups ($n = 5$ each): sham control group consisting of rats undergoing surgical procedure and cannulation without blood withdrawal, hemorrhage (Hem) group of rats undergoing hemorrhage without EF24 treatment, and Hem + EF24 group in which the rats received EF24 (0.4 mg/kg i.p.) with hemorrhage. For survival studies, additional six rats each were included in the Hem and Hem + EF24 groups. The hemorrhage was induced by withdrawing approximately 50% of circulating blood at the rate of 0.75 ml/min from rats anesthetized with 2% isoflurane in a stream of air (2 l/min). The total volume of blood was estimated at 5.7% of the total body weight. A fixed-volume hemorrhage protocol was used because it has been suggested that it imitates the clinical scenario more closely than the constant-pressure protocol (Bellamy et al., 1986). The blood pressure was digitally

monitored by instrumenting the rats to an iWorx data acquisition system (Dover, NH). The rats were heparinized with 100 units of heparin to prevent clotting. The hypovolemic rats were allowed to wake up and were transferred to a fresh cage. After 6 hours, the rats were euthanized with an overdose of SOMNASOL, Euthanasia-III Solution (Butler Schein Animal Health, Dublin, OH). The lung was harvested for immunoblotting and immunohistochemistry experiments. One-half of the lung was snap-frozen, whereas the other half was fixed in formalin.

Cytokines Assay. The plasma levels of cytokines were estimated by rat inflammation enzyme-linked immunosorbent assay (ELISA) strip for profiling TNF-α, IL-6, interferon-γ (IFN-γ), IL-1α, IL-1β, monocyte chemotactic protein-1 (MCP-1), regulated and normal T-cell expressed and secreted (RANTES) protein and macrophage inflammatory protein (MIP)-1α (Signosis, Sunnyvale, CA) following the manufacturer's instructions. In brief, 100 μl of standard, control, or sample was added to the designated wells and incubated for 1 hour at room temperature with gentle shaking. After washing the wells three times, 100 μl of biotin-conjugated antibody was added for 1 hour. The unreacted secondary antibody was washed off, and the wells were probed with streptavidin-horseradish peroxidase conjugate for 45 minutes. The wells were washed again, and 100 μl of substrate solution was added to generate the color. The reaction was stopped after 30 minutes, and the optical density was read at 450 nm.

The levels of TNF-α and IL-6 cytokines in lung tissue were estimated by rat inflammation ELISA strip for profiling TNF-α and IL-6 (Signosis, Sunnyvale, CA). The tissue samples were prepared by mincing the frozen lung tissues (75–100 mg) and incubating on ice for 30 minutes in 0.5 ml of ice-cold whole-cell lysate buffer consisting of 10% Nonidet P-40, 5 M NaCl, 1 M HEPES, 0.1 M ethylene glycol tetraacetic acid, 0.5 M ethylenediaminetetraacetic acid, 0.1 M phenylmethylsulfonyl fluoride, 0.2 M sodium orthovanadate, 1 M NaF, 2 μg/ml aprotinin, and 2 μg/ml leupeptin. The mixture was homogenized using a Dounce homogenizer and centrifuged at 14,000 rpm at 4°C for 10 minutes to obtain the test supernatants. The ELISA was performed according to the manufacturer's instructions.

Immunohistochemistry and Histopathology. The protein expression levels of phospho-NF-κB p65, COX-2, high mobility group box 1 (HMGB1), and TLR4 were assessed in lung tissues by using an immunohistochemistry kit from DakoCytomation (Carpinteria, CA). In brief, the tissue samples were fixed with paraformaldehyde and embedded in paraffin. After washing in phosphate-buffered saline, the slides were blocked with a protein-block solution for 20 minutes and incubated overnight with mouse monoclonal anti-rat phospho-NF-κB-p65 (Cell Signaling Technology, 3033), COX-2 (Santa Cruz Biotech, sc1746), HMGB1 (Cell Signaling Technology, 3935), and TLR4 (Cell Signaling Technology, 2219) antibodies at the dilutions of 1:200, 1:100, 1:100, and 1:200, respectively. The slides were washed and incubated with biotinylated link universal antiserum, followed by HRP-streptavidin conjugate. The slides were rinsed and the color was developed using 3,3-diaminobenzidine hydrochloride as a chromogen. Finally, the sections were rinsed in distilled water, counterstained with Mayer's hematoxylin solution, and mounted with DPX mounting medium for evaluation.

For histopathologic examination, the paraffin-embedded tissues were stained with hematoxylin and eosin stain. The slides were evaluated for morphologic changes and pathologic signatures of ischemia, inflammation, and any other abnormalities. The sections were observed with Olympus microscope IX701, and digital computer images were recorded using an Olympus DP70 camera.

Immunoblotting. The isolated frozen tissues (75–100 mg) were minced and incubated on ice for 30 minutes in 0.5 ml of ice-cold whole-cell lysate buffer consisting of 10% Nonidet P-40, 5 M NaCl, 1 M HEPES, 0.1 M ethylene glycol tetraacetic acid, 0.5 M ethylenediaminetetraacetic acid, 0.1 M phenylmethylsulfonyl fluoride, 0.2 M sodium orthovanadate, 1 M NaF, 2 μg/ml aprotinin, and 2 μg/ml leupeptin. The protein was extracted by homogenization using a Dounce homogenizer and centrifugation at 14,000 rpm at 4°C for 10 minutes. The proteins were fractionated by SDS-polyacrylamide gel electrophoresis,

electrotransferred to the nitrocellulose membranes, blotted with primary antibodies against phospho-NF-κB-p65 (3033; Cell Signaling Technology), TLR4 (2219; Cell Signaling Technology), COX-2 (sc1746; Santa Cruz Biotechnology), HMGB1 (3935; Cell Signaling Technology), inducible nitric-oxide synthase (iNOS) (ab15323; Abcam), heme oxygenase–1 (HO-1) (sc1797; Santa Cruz Biotechnology), nuclear factor (erythroid-derived 2)-like 2 (Nrf2) (2178-1; Epitomics), phospho-Nrf2 (2073-1; Epitomics), apurinic/apyrimidinic endonuclease (APE1) (4128; Cell Signaling Technology), superoxide dismutase–1 (SOD1) (2770; Cell Signaling Technology), and 8-oxoguanine glycosylase 1 (OGG1) (sc33181; Santa Cruz Biotech), followed by HRP-conjugated secondary antibody. The immunoreactive bands were detected by SuperSignal West Femto detection reagent (Thermo Fisher Scientific, Rockford, IL). To ensure equal protein loading in the wells, the membranes were stripped using a stripping solution containing 10% SDS and 0.5 M Tris and β-mercaptoethanol (35 μl/ml) at 60°C for 45 minutes, and reprobed with anti-actin antibody (A2066; Sigma-Aldrich; 1:1000 in TBST). The blots were imaged using Ultraquant image acquisition machine (Claremont, CA), and the densitometric readings for proteins were normalized with those of actin.

COX-2 Activity Assay. The cyclooxygenase activity in lung tissue homogenates of rats from three different treatment groups was determined using a 96-well COX fluorescent assay kit from Cayman Chemicals (Ann Arbor, MI). The manufacturer's directions were followed to estimate the COX activity in presence of COX-1 inhibitor (SC-560) supplied with the kit. The presence of COX-1 inhibitor eliminates the contribution of constitutively expressed COX-1 in total cyclooxygenase activity. The assay is based on the formation of a fluorescent compound resorufin (λ_{EX} 530–540 nm and λ_{EM} 585–595 nm) from the reaction between prostaglandin G2 and 10-acetyl-3,7-dihydroxyphenoxazine. The fluorescence values are directly related to COX-2's peroxidase activity that catalyzes the prostaglandin G2 and 10-acetyl-3,7-dihydroxyphenoxazine reaction. The pooled lung tissue homogenates from four rats/group were assayed as hexaplicates.

Myeloperoxidase Assay. The frozen lung samples were thawed, diced with a razor blade, and homogenized in 50 mM potassium phosphate buffer (pH 6.0). The homogenates were centrifuged at 10,000 rpm for 15 minutes, and the pellets were resuspended in 0.3 ml of phosphate buffer containing 50 mM hexadecyltrimethylammonium bromide (HTAB). After homogenizing for 30 seconds, the volume of mixture was made up to 1 ml by adding phosphate buffer (pH 7.4) without HTAB. The mixture was sonicated in a water bath for 20 seconds and snap-frozen in liquid nitrogen followed by thawing to room temperature. The sonication-freezing-thawing was repeated two more times before centrifuging the mixture at 10,000 rpm for 10 minutes. The aliquots of supernatants were diluted 1:2 and 1:10 with the HTAB-phosphate buffer and added with 30× the volume of phosphate buffer containing 0.167 mg/ml O-dianisidine dihydrochloride and 0.0005% hydrogen peroxide. The absorbance was monitored intermittently at 460 nm.

Data Analysis. Unless otherwise mentioned all the results were analyzed by one-way analysis of variance (ANOVA) applying the Bonferroni post-test using Prism software (GraphPad Software, Inc., San Diego, CA). $P < 0.05$ was considered statistically significant. The densitometry of immunoreactive bands was performed from three replicates using ImageJ 1.46r freeware (National Institutes of Health).

Results

In our previous reports, we described the potent NF-κB inhibitory activity of EF24 in an in vitro model (Vilekar et al., 2012). Here, we expanded our inquiry in an in vivo model of fixed-volume hemorrhage described elsewhere (Awasthi et al., 2007). After hemorrhage, the hematocrit values reduced from basal 44.1 ± 1.3 to 27.4 ± 1.1. For investigation of the hemorrhage-induced inflammation, we focused on lung because hemorrhagic shock often causes pulmonary dysfunction,

the severity of which correlates with the ensuing mortality. Lung is especially prone to injury in low flow states, and its propensity to the damage remains even after volume and oxygen deficits are corrected.

Histologic Injury. The acute histopathologic consequences of hemorrhage in lung are shown in Fig. 1A. The blood loss initiated significant morphologic changes in lung. We found that after hemorrhage, there was severe pulmonary congestion and loss of alveolar integrity. The hemorrhaged lung was characterized by thickening of alveolar epithelium and interstitial exudates. These changes are ascribed to the inflammatory process and hemorrhage-induced cytokine storm, collectively described as generalized interstitial pneumonitis. There was substantial staining for inflammatory cell infiltration. Whether the pulmonary changes were associated with neutrophil infiltration was assessed by determining myeloperoxidase activity in lung tissue lysate. The treatment with EF24 markedly ameliorated
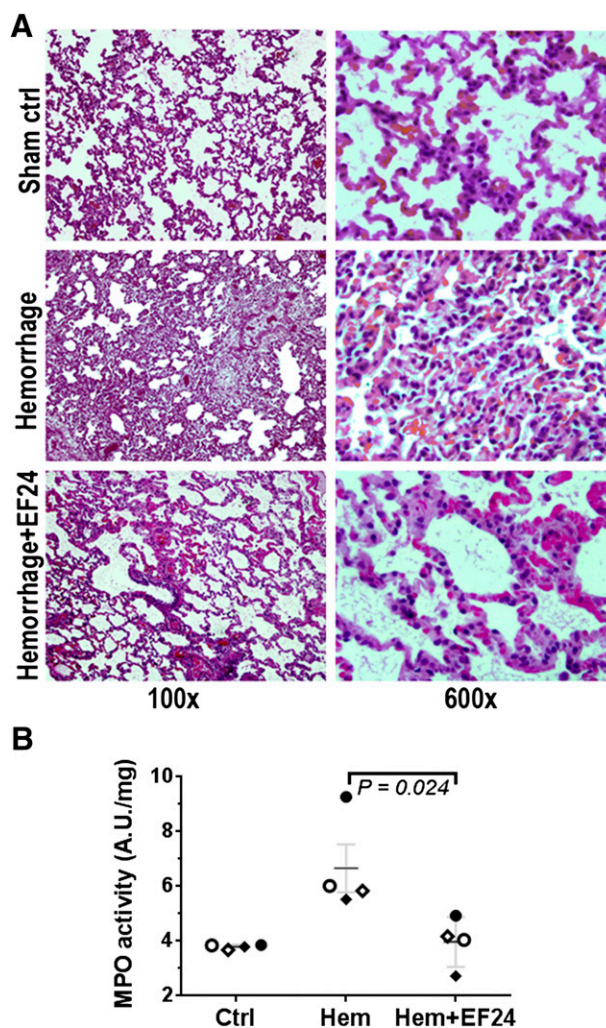

Fig. 1. (A) Histopathology of lung tissues from a representative set of rats, showing that EF24 prevented hemorrhage-induced damages. The rats in the sham control group were subjected to surgery but no blood loss, whereas hemorrhaged groups were bled 50% of blood calculated on the basis of body weight (5.7 ml/100 g). The tissue slides were stained with hematoxylin and eosin, and digital micrographs were obtained at 100× or 600× magnification. (B) Myeloperoxidase activity in lung tissue from control (Ctrl), hemorrhage (Hem), and hemorrhage + EF24 (Hem + EF24) groups. The dark horizontal lines represent the mean values of the respective groups, shown with S.E.M.

the post-hemorrhage morphologic changes and inflammatory cell infiltration. The hemorrhage-induced increase in myeloperoxidase activity was also prevented by EF24 treatment (Fig. 1B).

EF24 Inhibits Hemorrhage-Induced NF-κB Phosphorylation. The transcriptional activity of NF-κB is regulated by the Ser536 phosphorylation of p65 subunit by IκB kinases (Sakurai et al., 2003). Therefore, the tissue expression of phospho-p65 subunit of NF-κB is a marker of NF-κB activation. In our fixed-volume hemorrhage model, the immunohistochemical examination revealed a clear induction of phospho-NF-κB p65 in hemorrhaged lung tissue. The treatment with EF24 prevented this induction in a significant manner (Fig. 2, A and B). Furthermore, the tissue homogenates were immunoblotted for phospho-NF-κB p65, which confirmed the hemorrhage-induced upregulation of phospho-NF-κB p65 and its recovery by EF24 treatment (Fig. 2, C and D).

EF24 Suppresses Hemorrhage-Induced TLR4 Expression. TLR4 plays an important role in hemorrhage-induced inflammation. TLR4-ligand interaction could activate the NF-κB-dependent as well as NF-κB-independent inflammatory pathways. Therefore, we investigated the effect of EF24 on the tissue expression of TLR4. The immunohistochemical staining and immunoblotting of lysates from lung tissues demonstrated that hemorrhage increased the expression levels of TLR4. EF24 treatment suppressed the hemorrhage-induced TLR4 expression (Fig. 3). The effects of hemorrhage and EF24 treatment on TLR4 expression in lung were unambiguous.

EF24 Suppresses Hemorrhage-Induced Circulating Cytokines. During both acute and chronic inflammatory processes, a variety of soluble factors belonging to the cytokine/chemokine family are involved in the systemic responses to inflammation. Among our panel of eight inflammatory markers, TNF-α, IL-6, IL-1α, and IL-1β constitute the proinflammatory cytokine category, whereas IFN-γ is considered as an anti-inflammatory cytokine. Table 1 shows the effect of EF24 on the expression levels of these cytokines. The rats in all three groups (sham control, Hem, and Hem + EF24) were sampled at zero time and after 6 hours of blood withdrawal. The end of the withdrawal period (approximately 12 minutes after the initiation of withdrawal) was taken as the zero time. It is apparent that hemorrhage induced the serum levels of TNF-α, IL-6, IFN-γ, IL-1α, and IL-1β. The treatment of animals with single i.p. injection of EF24 (0.4 mg/kg) significantly prevented the hemorrhage-induced rise in serum cytokine levels.

Coordinating closely with the inflammatory cytokines in hemorrhage-induced inflammation are the chemokines, such as MCP-1, RANTES, and MIP-1α. As shown in Table 1, although hemorrhage by itself did not significantly increase their levels, the EF24 treatment significantly suppressed these chemokines below their basal levels.

EF24 Inhibits Hemorrhage-Induced COX-2 Expression and Activity. The eicosanoids generated from COX-2 activation are important players in the manifestation of inflammatory pathology. We show by immunohistochemical (Fig. 4, A and B) and immunoblotting (Fig. 4, C and D) evidence
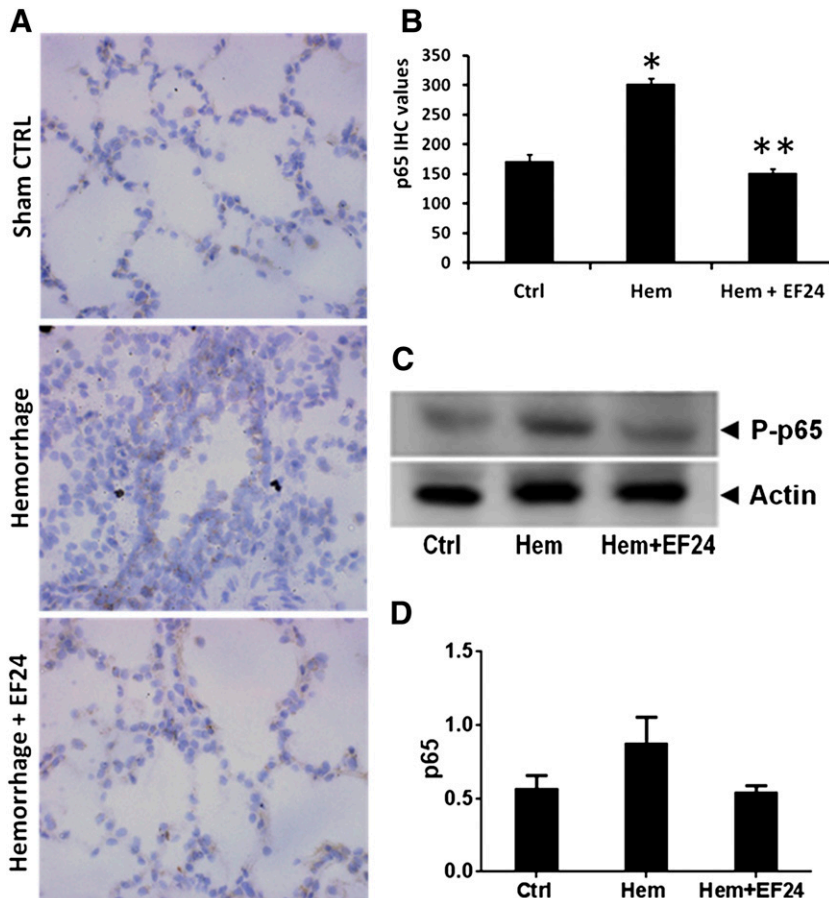

Fig. 2. (A) Immunohistochemical (IHC) analysis of phospho-NF-κB p65 expression in lung tissues of rats subjected to sham surgery (Ctrl), hemorrhage (Hem), and hemorrhage with EF24 administration (Hem + EF24). The pictures are a representative set from three similar sets. The light blue stain represents the degree of expression of phospho-p65. (B) Quantitation of IHC values (*P < 0.05 versus control; **P < 0.05 versus hemorrhage). (C) The protein expression of phospho-NF-κB p65 as observed by immunoblotting. To demonstrate equal loading, the membranes were stripped and reprobed with anti-β-actin antibody. (D) Actin-normalized densitometry of the immunoblots.
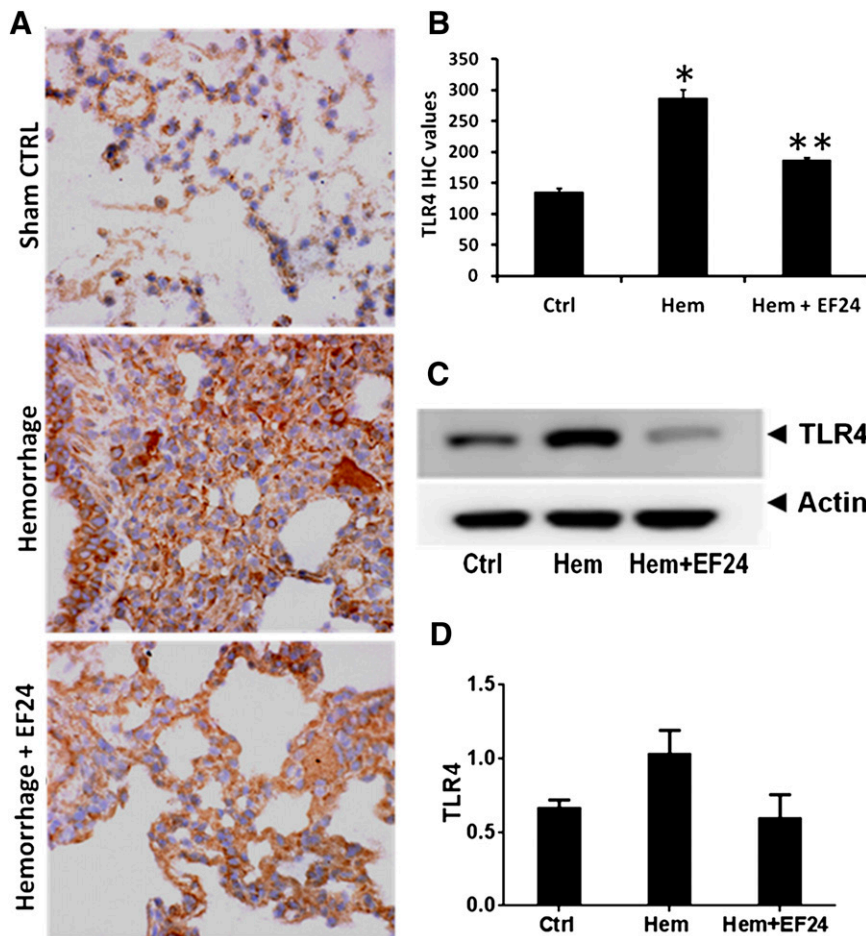
Fig. 3. (A) Immunohistochemical (IHC) analysis of TLR4 expression in lung tissues of rats subjected to sham surgery (Ctrl), hemorrhage (Hem), and hemorrhage with EF24 administration (Hem + EF24). The pictures are a representative set from three similar sets. The light blue stain represents the degree of expression of TLR4. (B) Quantitation of IHC values (*$P < 0.05$ vs. control; **$P < 0.05$ vs. hemorrhage). (C) The protein expression of TLR4 as observed by immunoblotting. To demonstrate equal loading, the membranes were stripped and reprobed with anti-β-actin antibody. (D) Actin-normalized densitometry of TLR4 immunoblots.

that EF24 treatment inhibited the hemorrhage-induced COX-2 expression in lung tissue. To further investigate whether the reduction in COX-2 expression is reflected in the corresponding decrease in its enzyme activity, we analyzed COX-2 activity in the pooled lung tissue lysates of hemorrhaged and EF24-treated rats. Figure 5 shows that EF24 treatment indeed suppressed the hemorrhage-induced increase in COX-2 activity in the lung tissue.

EF24 Reduces Hemorrhage-Induced Pulmonary HMGB1 Levels. In addition to the usual cytokines, recent studies have indicated that HMGB1 could also function as an inflammatory cytokine, especially in hemorrhagic shock (Parrish and Ulloa, 2007). It acts as a DAMP released in the extracellular milieu by trauma-afflicted cells. Because it is an early mediator of inflammation in sterile tissue injury (Peltz et al., 2009), its expression is an important criterion in assessing the ischemic injury caused by hemorrhage. We evaluated HMGB1 expression in lung tissue by immunohistochemistry (Fig. 6, A and B) and immunoblotting (Fig. 6, C and D) of the tissue homogenates. We found that hemorrhage significantly induced the HMGB1 levels and that EF24 treatment reduced the hemorrhage-induced HMGB1 expression.

TABLE 1

Effect of EF24 administration on serum levels of inflammatory cytokines

Cytokine	Mean ± S.D.		
	Sham Control	Hemorrhage	Hemorrhage + EF24
TNF-α (ng/ml)	0.284 ± 0.029	0.385 ± 0.014***	0.206 ± 0.006***,###
IL-6 (ng/ml)	0.617 ± 0.017	0.804 ± 0.004***	0.417 ± 0.012***,###
IFN-γ (ng/ml)	0.646 ± 0.018	0.799 ± 0.082**	0.469 ± 0.031**,###
IL-1α (ng/ml)	0.114 ± 0.012	0.163 ± 0.007***	0.065 ± 0.005***,###
IL-1β (ng/ml)	0.810 ± 0.007	1.007 ± 0.077***	0.325 ± 0.029***,###
MCP-1 (ng/ml)	0.285 ± 0.037	0.311 ± 0.012 NS	0.203 ± 0.017**,###
RANTES (ng/ml)	0.281 ± 0.064	0.267 ± 0.026 NS	0.168 ± 0.013*,#
MIP-1α (ng/ml)	0.248 ± 0.012	0.270 ± 0.017 NS	0.161 ± 0.009***,###

NS, not significant.
* and #$P < 0.05$ vs. sham control and hemorrhage groups, respectively.
** and ##$P < 0.01$ vs. sham control and hemorrhage groups, respectively.
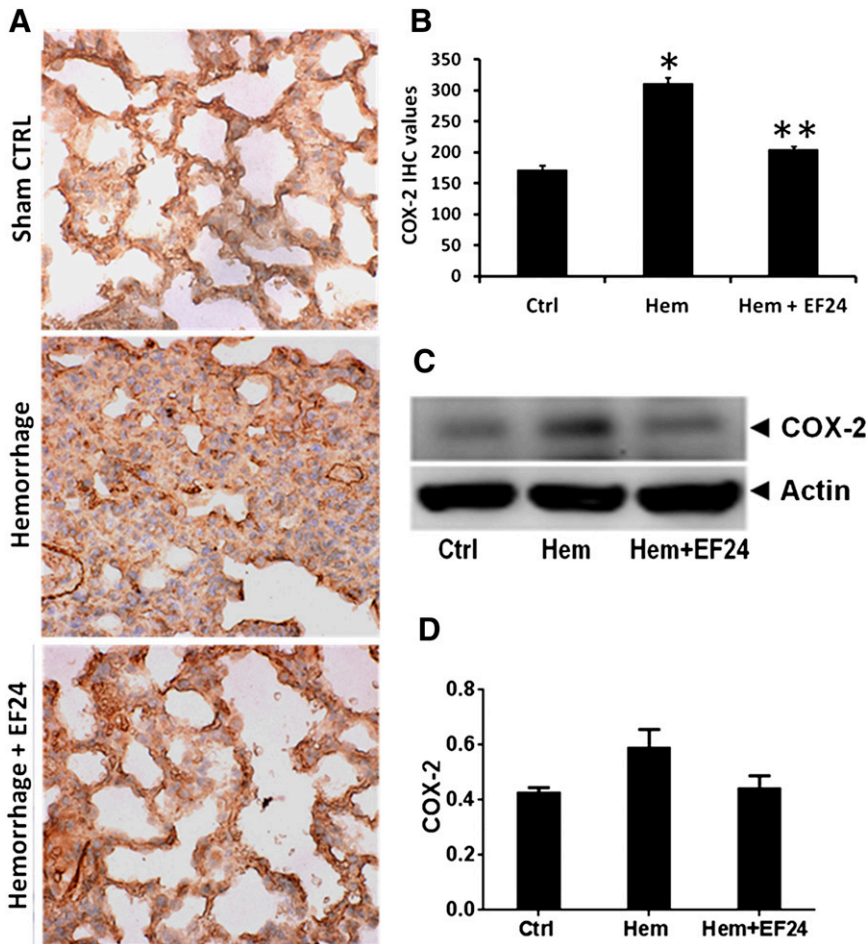*** and ###$P < 0.001$ vs. sham control and hemorrhage groups, respectively.

Fig. 4. (A) Immunohistochemical (IHC) analysis of COX-2 expression in lung tissues of rats subjected to sham surgery (Ctrl), hemorrhage (Hem), and hemorrhage with EF24 administration (Hem + EF24). The pictures are a representative set from three similar sets. The light blue stain represents the degree of expression of COX-2. (B) Quantitation of IHC values (*$P < 0.05$ vs. control; **$P < 0.05$ vs. hemorrhage). (C) The protein expression of COX-2 as observed by immunoblotting. To demonstrate equal loading, the membranes were stripped and reprobed with anti-β-actin antibody. (D) Actin-normalized densitometry of COX-2 immunoblots.

EF24 Curbs Hemorrhage-Induced iNOS Expression and HO-1. The production of nitric oxide and eicosanoids constitutes a chemical network that orchestrates the overall clinico-pathologic symptoms of inflammation. The inducible form of nitric oxide synthase is under the transcriptional control of NF-κB. As shown in Fig. 7A, the treatment of rats
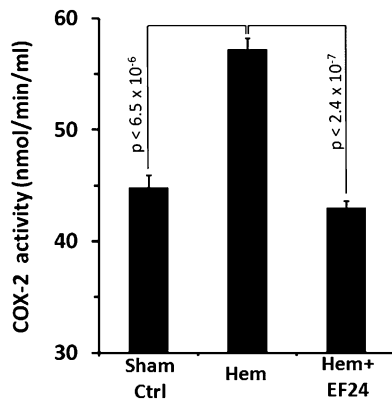

Fig. 5. EF24 reduces lung-associated tissue COX-2 activity in hemorrhaged animals. COX-2 activity was determined by the amount of fluorescent resorufin generated by cyclooxygenase's peroxidase-catalyzed reaction between prostaglandin G2 and 10-acetyl-3,7-dihydroxyphenoxazine in the presence of COX-1 inhibitor SC-560. H, hemorrhage; H + EF24, hemorrhage plus EF24.

with EF24 reduced the hemorrhage-induced increase in iNOS expression. Similar to iNOS, the elevated expression of HO-1 is also an endogenous protective mechanism against oxidative stress (Tamion et al., 2001). We monitored HO-1 expression in lung tissue by immunoblotting (Fig. 7B). The effect of hemorrhage on the expression of HO-1 in lung tissue was not conclusively evident. EF24 treatment appeared to reduce the HO-1 expression to a level below the levels observed after hemorrhage, but the changes were not statistically significant.

EF24 Generates a Protective Response Against Oxidative Stress. As a consequence of oxidative stress after blood loss, another transcriptional regulator, Nrf2, is upregulated in hemorrhage-associated inflammation. As shown in Fig. 8, hemorrhage resulted in a moderate increase in Nrf2 phosphorylation compared with the basal level, implying a modest induction of protective antioxidant response to the hemorrhage-induced oxidative stress. EF24 administration markedly enhanced Nrf2 activation over and above the hemorrhage-induced response (Fig. 8). In line with the expectations, EF24 treatment also significantly increased the expression of Nrf2-regulated SOD1, OGG1, and APE1 (Fig. 8). SOD, APE1, and OGG are a few of the protective enzymes from disparate classes that are induced under oxidative stress, with a common purpose of maintaining reactive oxygen species at benign levels.

EF24 Improves Hemodynamics and Survival of Hemorrhaged Rats. Whereas the biochemical markers of inflammation and oxidative stress response suggest significant
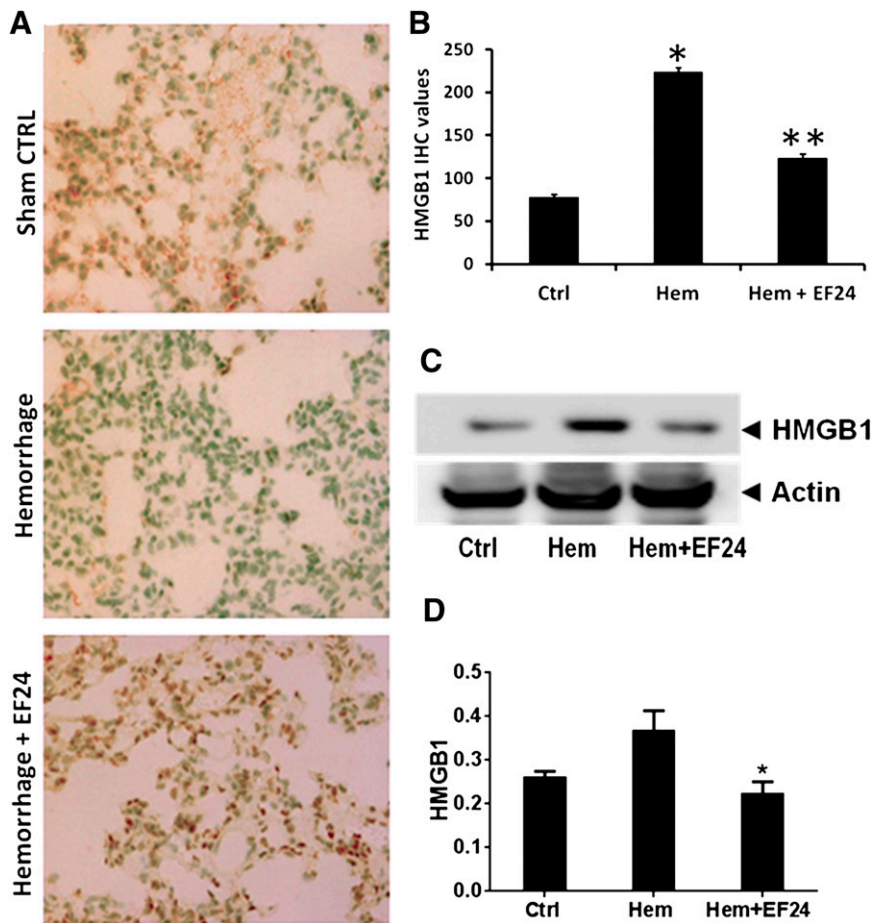
Fig. 6. EF24 decreases lung tissue–associated HMGB1 expression. (A) Immunohistochemical analysis of HMGB1 expression in lung tissues of rats subjected to sham surgery (Ctrl), hemorrhage (Hem), and hemorrhage with EF24 administration (Hem + EF24). The pictures are a representative set from three similar sets. (B) Quantitation of IHC values (*$P < 0.05$ vs. control; **$P < 0.05$ vs. hemorrhage). (C) The protein expression of HMGB1 as observed by immunoblotting. To demonstrate equal loading, the membranes were stripped and reprobed with anti-β-actin antibody. (D) Actin-normalized densitometry of HMGB1 immunoblots ($P < 0.05$ vs. hemorrhage).

anti-inflammatory benefits of EF24 administration in hemorrhaged rats, the eventual therapeutic outcome is measured in terms of post-hemorrhage survival. We recruited additional rats to study the effect of EF24 on mean arterial blood pressure (MAP) (Fig. 9A) and 6-hour survival (Fig. 9B) after hemorrhage. As expected, hemorrhage caused a significant decline in MAP. The MAP readings of the surviving rats at 6 hours showed that EF24-treatment recovered MAP to almost
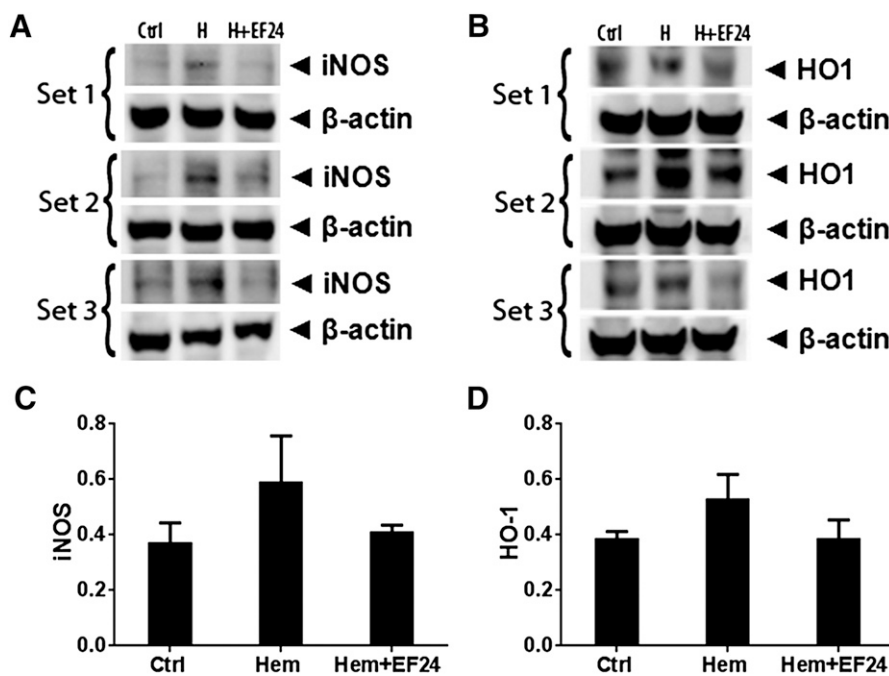

Fig. 7. Triplicate Western blots of (A) iNOS) and (B) HO-1 expression in lung tissues of rats subjected to sham surgery (Ctrl), hemorrhage (Hem), and hemorrhage with EF24 administration (Hem + EF24). (C and D) are densitometry of iNOS and HO-1 immunoblots, respectively.
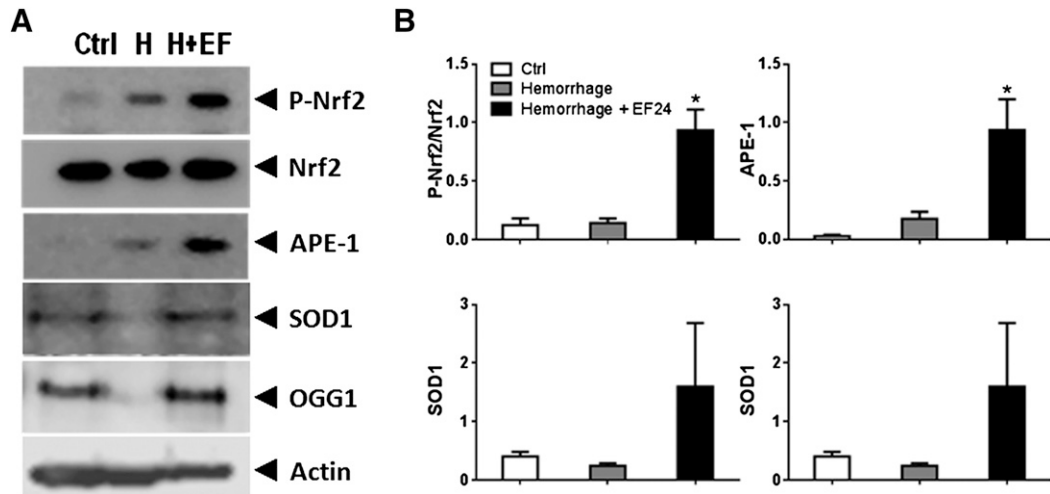
Fig. 8. (A) Representative immunoblots of select markers of Nrf2-mediated protective response. (B) Densitometric analyses of immunoblots.

70% of baseline levels, which was significantly better than the recovery observed in control rats treated with an equal volume of saline (50 μl). The survival data (Fig. 9B) demonstrated that EF24 significantly improved the survival of hemorrhaged rats ($P < 0.05$). Whereas 4/11 (36%) of rats belonging to the saline group survived the 6-hour deadline, 9/12 (75%) of rats in the EF24 group survived for 6 hours. The times of deaths in the saline group were also observed to be much earlier than those in the EF24 group. All casualties in the saline group occurred within 1.5 hours of hemorrhage (1.2 $\pm$ 0.28 hours), but the causalities in the EF24 group were substantially delayed (2.2 $\pm$ 0.6 hours).

Overall, the results indicate that EF24 treatment antagonizes the hemorrhage-induced inflammatory pathways in a pluripotent fashion (Fig. 10). At the same time, it induces the protective antioxidant response regulated by Nrf2. The net benefit of these salutary effects of EF24 was observed in the increase in survival of rats hemorrhaged by 50% of their circulating blood volume.

Discussion

Despite the importance of controlling inflammation in the victims of HS, a suitable anti-inflammatory therapeutic for this indication is conspicuously missing. The systemic use of COX inhibitors is not widely practiced because their undesirable cardiovascular side effects may aggravate the pathology of HS (Heim and Broich, 2006; Marwali and Mehta, 2006). To address hemorrhage-associated inflammation in a comprehensive manner, a strategy of modulating the transcriptional control of inflammatory processes has been suggested (Wu, 2006). The NF-κB family of transcription factors plays a pivotal role in post-hemorrhage inflammation, because it regulates more than 60 proinflammatory genes involved in myriad of inflammation-related processes (Villavicencio and Billiar, 1999). Its role has also been linked to the hemodynamic changes observed during shock (Doursout et al., 2009), and it serves as an important pivot in the signaling of IL-1R superfamily, which includes TLR4. The convergence of so many different inflammation signaling pathways on a single target provides an opportunity to address several proinflammatory sequels by NF-κB

inhibition. Our previous study in dendritic cells suggested that EF24 modulates the inflammatory immune responses and potently inhibits NF-κB (Vilekar et al., 2012). The in vivo data presented herein demonstrate that EF24 could suppress expression of NF-κB-regulated biomarkers of inflammation in lung and improve survival in HS.
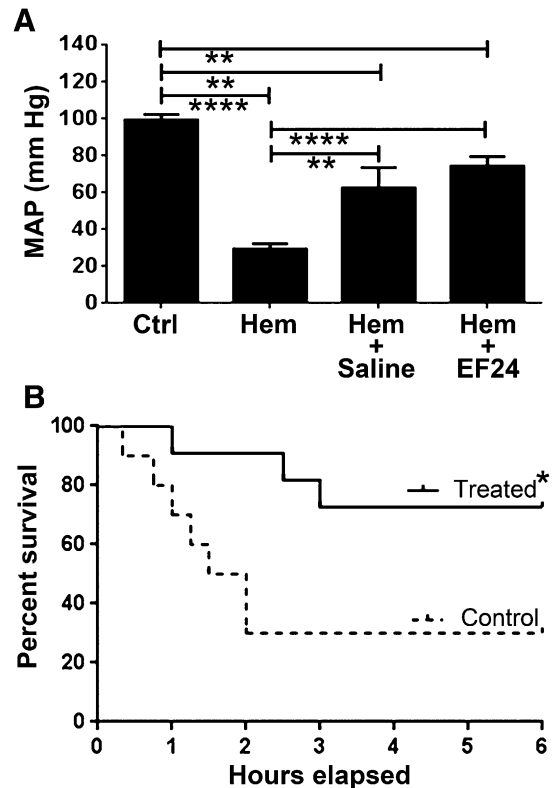

Fig. 9. EF24 treatment significantly improves hemodynamics and survival in hemorrhaged rats. (A) Mean arterial pressure in rats treated with EF24 or vehicle control (saline). The blood pressure was measured after 5 minutes and 6 hours of hemorrhage. Statistical t test was used to compare different groups (n = 6/group, $P < 0.05$ was accepted as statistically significant). (B) Kaplan-Meier survival curve. Log-rank (Mantel-Cox) test was used to determine the significance between the two groups: EF24-treated and control. $P < 0.05$ was accepted as statistically significant.
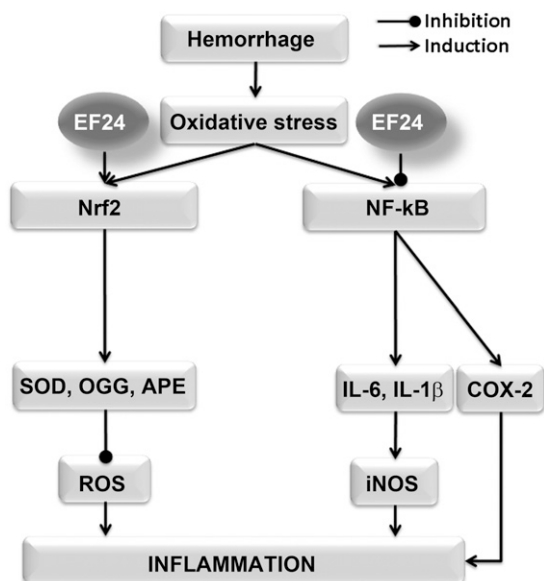
Fig. 10. The pleiotropic effects of EF24 against inflammation. The oxidative stress generated by blood loss recruits Nrf2 response on one hand and the TLR4/NF-κB axis on the other hand. Both pathways are part of a protective response initiated by the hypoperfusion-induced tissue injury. Whereas the Nrf2-mediated antioxidant response in severe hemorrhage may not be sufficient to salvage the tissue, NF-κB-driven inflammatory cascade may quickly attain exaggerated levels detrimental to the organism as a whole. The salutary effects of EF24 treatment in hemorrhage appear to be because it enhances the Nrf2-mediated antioxidant response and suppresses the NF-κB-driven inflammation.

The accessible markers of activated NF-κB pathway in HS are the levels of serum cytokines and chemokines that have a strong correlation with the overall clinical outcome (Roumen et al., 1993). Major cytokines that participate in response to trauma include TNF-α, IL-1β, and IL-6 (Namas et al., 2009). Infliximab, a monoclonal antibody against TNF-α, also protects organs from the I/R-induced damage (Guzel et al., 2012; Pergel et al., 2012; Tasdemir et al., 2012). However, the neutralization of an effector molecule does not appear to be an efficient strategy against HS-associated inflammation. At the same time, pentoxyfylline- or infliximab-driven TNF-α antagonism undermines the multifaceted nature of the systemic inflammatory response syndrome.

Unlike cytokines, the chemokines and their receptors are more critically involved in the pathogenesis of I/R injury phase, and chemokine antagonists have been found useful in minimizing leukocyte infiltration and preventing the postischemic organ dysfunction (Takami et al., 2001; Jo et al., 2003; Krishnadasan et al., 2004; Reichel et al., 2006). The model used in our study does not serve as a model of I/R injury. As a consequence, we could not find any significant change in the levels of MIP-1α, MCP-1, or RANTES after hemorrhage (Table 1). Nonetheless, the ability of EF24 to significantly reduce the levels of MIP-1α, MCP-1, and RANTES below the basal levels suggests its potential benefit in I/R injury. Another interesting effect of EF24 was on HMGB1, a DAMP molecule with cytokine-like actions in hemorrhage-induced inflammation. HMGB1 binds to TLR4 and interacts with the receptor for advanced glycation end products, TLR2, TLR9, and CD24 (Andersson and Tracey, 2011). As a DAMP, it is juxtaposed at the intersection of sterile and infectious inflammation, providing a link between

sterile tissue injury and the activation of innate immune responses (Andersson and Tracey, 2011). As such, the suppressive effect of EF24 on pulmonary HMGB1 expression may have significant therapeutic implications, because the HMGB1 inhibitor glycyrrhizin has been noted to prevent I/R-mediated tissue injury (Mabuchi et al., 2009; Ogiku et al., 2011).

Besides controlling the expression of proinflammatory cytokines, NF-κB also functions upstream of the *COX-2* gene (Tsatsanis et al., 2006). Although *COX-2* has long been identified as one of the early genes expressed in HS and I/R injury (Hierholzer and Billiar, 2001; Rajnik et al., 2002), we could not find any report on pharmacotherapy of "sterile" HS with selective COX-2 inhibitors (e.g., celecoxib). Celecoxib, however, has been reported to reduce the deleterious consequences of sepsis in a mouse model of trauma-hemorrhage (Knoferl et al., 2001). In our model of HS, EF24 treatment reversed the effect of hemorrhage on COX-2 expression. Unlike celecoxib, which directly influences the activity of COX-2, the reduction in lung COX-2 activity by EF24 appears to be the result of a decrease in total COX-2 expression at transcriptional levels. Yet another NF-κB-regulated proinflammatory molecule is iNOS. Small amounts of NO generated by endothelial NOS are protective in I/R injury (Abu-Amara et al., 2012), but the induction of iNOS results in the generation of large and toxic amounts of NO. The generated NO reacts with superoxide radicals to form a highly reactive peroxynitrite radical, which is implicated in an irreversible damage in HS and I/R injury (Guzik et al., 2003). EF24 appears to suppress iNOS induction in a substantial manner, perhaps by its NF-κB inhibitory activity.

Similar to NF-κB, Nrf2 is another cytoplasm-bound transcription factor that undergoes phosphorylation-dependent activation and nuclear translocation in response to oxidative stress (Itoh et al., 1997). The activated Nrf2 binds to the antioxidant response element within the promoter region of many protective enzymes and activates their transcription (Jaiswal, 2004; D'Autreaux and Toledano, 2007). A sufficient level of Nrf2-mediated antioxidant response is necessary for the effective resolution of hemorrhage-induced oxidative stress (Kong et al., 2010). In our model, hemorrhage was found to induce Nrf2 response to modest levels, but the protective response was not sufficient to subdue the proinflammatory IL-1R pathways (unpublished data) and inflammatory markers such as iNOS (Fig. 7). On the other hand, EF24 induced the level of hemorrhage-induced Nrf2 response, which appeared to have neutralized the proinflammatory response, indicated by lower IL-1R1 signaling (unpublished data) and iNOS expression (Fig. 7). When effective, the Nrf2-regulated enzymes work with NF-κB and apoptotic pathways to preserve the growth characteristics of cells. SOD1, APE1, and OGG1 are three important Nrf2-regulated enzymes responsible for negotiating the effects of highly destructive superoxide radicals on cellular structure and function (Tell et al., 2005; Bravard et al., 2006). The EF24-induced expression of these enzymes is an evidence of protective consequences of EF24 administration in HS. Another Nrf2-regulated protective enzyme upregulated in hemorrhage and I/R injury is HO-1. However, we found that EF24 treatment did not increase the expression of HO-1 in lung tissue. It is difficult to satisfactorily explain this contradiction because there exist a plethora of data showing positive correlation between Nrf2 activation and HO-1 expression in similar experimental settings (Takahashi et al., 2009; Ganster

et al., 2010). Upon further literature exploration, we found a few reports suggesting that HO-1 expression in lung could be controlled by NF-κB (Lin et al., 2007; Li et al., 2008; van Berlo et al., 2010). Moreover, the attenuation of lung injury by pentoxyfylline administration has also been found to be associated with reduction in HO-1 expression in a rat model of HS (Deree et al., 2007a; Deree et al., 2007b). Whether this phenomenon is dependent on the resolution of inflammatory and oxidative stress, secondary to the NF-κB inhibition remains a subject of further investigation. It is also noteworthy that the stress-induced HO-1 in organs that are not directly involved in erythrocyte or hemoglobin turnover could be injurious (Takahashi et al., 2007). This is supported by the observation that the induction of pulmonary HO-1 results in the development of lung dysfunction after hemorrhagic shock and resuscitation (Chen et al., 2009).

Conclusions

From the results of this study, we conclude that EF24 suppresses inflammatory responses after severe hemorrhage and improves survival. However, one notable limitation of this study is the need for data on the efficacy of EF24 administration after hemorrhage. Nonetheless, the effects of EF24 in a small-volume administration, without concomitant volume and/or oxygen deficit correction, are encouraging. As such, it is important to investigate EF24 further in a more relevant model. Other small molecules, such as valproate and ethyl pyruvate (EP), have been investigated for pharmacologic resuscitation in HS (Kao and Fink, 2010; Cotton, 2011). Both the mechanistic basis and the therapeutic dose of EF24 are different from those of valproate and EP. The anti-inflammatory activity of EF24 in lung is most likely dependent on its ability to inhibit NF-κB activation. The efficacy of EP depends on the reduction of oxidative stress secondary to reactive oxygen species scavenging (Kao and Fink, 2010), whereas valproate inhibits histone deacetylase (Lin et al., 2007) and modulates the β-catenin survival pathway (Li et al., 2008) in HS. Both EP and valproate are reportedly used at approximately 200 mg/kg body weight in combination with conventional resuscitation fluids, whereas EF24 was administered at a dose of 0.4 mg/kg body weight without accompanying resuscitation fluid. Recently, a hydrogen sulfide donor, NaHS, (1.57 mg/kg body weight) has also been found to possess cardioprotective effects ascribed to NF-κB inhibition in a rat HS model (Gao et al., 2012).

Authorship Contributions

Participated in research design: Yadav, Awasthi.
Conducted experiments: Yadav, Sahoo, Awasthi.
Contributed new reagents or analytic tools: Awasthi.
Performed data analysis: Awasthi, Yadav, Roberts.
Wrote or contributed to the writing of the manuscript: Awasthi, Yadav, Roberts.

References

Abu-Amara M, Yang SY, Seifalian A, Davidson B, and Fuller B (2012) The nitric oxide pathway—evidence and mechanisms for protection against liver ischaemia reperfusion injury. *Liver Int* 32:531–543.

Andersson U and Tracey KJ (2011) HMGB1 is a therapeutic target for sterile inflammation and infection. *Annu Rev Immunol* 29:139–162.

Awasthi V, Yee SH, Jerabek P, Goins B, and Phillips WT (2007) Cerebral oxygen delivery by liposome-encapsulated hemoglobin: a positron-emission tomographic evaluation in a rat model of hemorrhagic shock. *J Appl Physiol* 103:28–38.

Bellamy RF, Maningas PA, and Wenger BA (1986) Current shock models and clinical correlations. *Ann Emerg Med* 15:1392–1395.

Bone RC (1996) Immunologic dissonance: a continuing evolution in our understanding of the systemic inflammatory response syndrome (SIRS) and the multiple organ dysfunction syndrome (MODS). *Ann Intern Med* 125:680–687.

Bravard A, Vacher M, Gouget B, Coutant A, de Boisferon FH, Marsin S, Chevillard S, and Radicella JP (2006) Redox regulation of human OGG1 activity in response to cellular oxidative stress. *Mol Cell Biol* 26:7430–7436.

Chen C, Wang Y, Zhang Z, Wang C, and Peng M (2009) Toll-like receptor 4 regulates heme oxygenase-1 expression after hemorrhagic shock induced acute lung injury in mice: requirement of p38 mitogen-activated protein kinase activation. *Shock* 31: 486–492.

Cotton BA (2011) Alternative fluids for prehospital resuscitation: "pharmacological" resuscitation fluids. *J Trauma* 70(5, Suppl)S30–S31.

D'Autréaux B and Toledano MB (2007) ROS as signalling molecules: mechanisms that generate specificity in ROS homeostasis. *Nat Rev Mol Cell Biol* 8:813–824.

Deree J, de Campos T, Shenvi E, Loomis WH, Hoyt DB and Coimbra R (2007a) Hypertonic saline and pentoxifylline attenuates gut injury after hemorrhagic shock: the kinder, gentler resuscitation. *J Trauma* 62:818-827; discussion 827-818.

Deree J, Martins J, de Campos T, Putnam JG, Loomis WH, Wolf P, and Coimbra R (2007b) Pentoxifylline attenuates lung injury and modulates transcription factor activity in hemorrhagic shock. *J Surg Res* 143:99–108.

Doursout M-FJ, Liang YY, Uray KS, Pati S, Matijevic N and Holcomb JB (2009) Role of the NF-κB pathway in rats subjected to moderate hemorrhage. *FASEB J* 23 (Suppl.):LB380.

Fukunaga K, Kohli P, Bonnans C, Fredenburgh LE, and Levy BD (2005) Cyclooxygenase 2 plays a pivotal role in the resolution of acute lung injury. *J Immunol* 174:5033–5039.

Ganster F, Burban M, de la Bourdonnaye M, Fizanne L, Douay O, Loufrani L, Mercat A, Calès P, Radermacher P, and Henrion D, et al. (2010) Effects of hydrogen sulfide on hemodynamics, inflammatory response and oxidative stress during resuscitated hemorrhagic shock in rats. *Crit Care* 14:R165–R176.

Gao C, Xu DQ, Gao CJ, Ding Q, Yao LN, Li ZC, and Chai W (2012) An exogenous hydrogen sulphide donor, NaHS, inhibits the nuclear factor κB inhibitor kinase/nuclear factor κb inhibitor/nuclear factor-κB signaling pathway and exerts cardioprotective effects in a rat hemorrhagic shock model. *Biol Pharm Bull* 35: 1029–1034.

Guzel A, Kanter M, Guzel A, Pergel A, and Erboga M (2012) Anti-inflammatory and antioxidant effects of infliximab on acute lung injury in a rat model of intestinal ischemia/reperfusion. *J Mol Histol* 43:361–369.

Guzik TJ, Korbut R, and Adamek-Guzik T (2003) Nitric oxide and superoxide in inflammation and immune regulation. *J Physiol Pharmacol* 54:469–487.

Heim HK and Broich K (2006) Selective COX-2 inhibitors and risk of thromboembolic events - regulatory aspects. *Thromb Haemost* 96:423–432.

Hierholzer C and Billiar TR (2001) Molecular mechanisms in the early phase of hemorrhagic shock. *Langenbecks Arch Surg* 386:302–308.

Itoh K, Chiba T, Takahashi S, Ishii T, Igarashi K, Katoh Y, Oyake T, Hayashi N, Satoh K, and Hatayama I, et al. (1997) An Nrf2/small Maf heterodimer mediates the induction of phase II detoxifying enzyme genes through antioxidant response elements. *Biochem Biophys Res Commun* 236:313–322.

Jaiswal AK (2004) Nrf2 signaling in coordinated activation of antioxidant gene expression. *Free Radic Biol Med* 36:1199–1207.

Jo N, Wu GS, and Rao NA (2003) Upregulation of chemokine expression in the retinal vasculature in ischemia-reperfusion injury. *Invest Ophthalmol Vis Sci* 44:4054–4060.

Kao KK and Fink MP (2010) The biochemical basis for the anti-inflammatory and cytoprotective actions of ethyl pyruvate and related compounds. *Biochem Pharmacol* 80:151–159.

Karin M, Lawrence T, and Nizet V (2006) Innate immunity gone awry: linking microbial infections to chronic inflammation and cancer. *Cell* 124:823–835.

Kasinski AL, Du Y, Thomas SL, Zhao J, Sun SY, Khuri FR, Wang CY, Shoji M, Sun A, and Snyder JP, et al. (2008) Inhibition of IkappaB kinase-nuclear factor-kappaB signaling pathway by 3,5-bis(2-flurobenzylidene)piperidin-4-one (EF24), a novel monoketone analog of curcumin. *Mol Pharmacol* 74:654–661.

Knöferl MW, Diodato MD, Schwacha MG, Cioffi WG, Bland KI, and Chaudry IH (2001) Cyclooxygenase-2-mediated regulation of Kupffer cell interleukin-6 production following trauma-hemorrhage and subsequent sepsis. *Shock* 16:479–483.

Kong X, Thimmulappa R, Kombairaju P, and Biswal S (2010) NADPH oxidase-dependent reactive oxygen species mediate amplified TLR4 signaling and sepsis-induced mortality in Nrf2-deficient mice. *J Immunol* 185:569–577.

Krishnadasan B, Farivar AS, Naidu BV, Woolley SM, Byrne K, Fraga CH, and Mulligan MS (2004) Beta-chemokine function in experimental lung ischemia-reperfusion injury. *Ann Thorac Surg* 77:1056–1062.

Lagisetty P, Vilekar P, Sahoo K, Anant S, and Awasthi V (2010) CLEFMA-an antiproliferative curcuminoid from structure-activity relationship studies on 3,5-bis (benzylidene)-4-piperidones. *Bioorg Med Chem* 18:6109–6120.

Li Y, Liu B, Sailhamer EA, Yuan Z, Shults C, Velmahos GC, deMoya M, Shuja F, Butt MU, and Alam HB (2008) Cell protective mechanism of valproic acid in lethal hemorrhagic shock. *Surgery* 144:217–224.

Lin T, Chen H, Koustova E, Sailhamer EA, Li Y, Shults C, Liu B, Rhee P, Kirkpatrick J, and Alam HB (2007) Histone deacetylase as therapeutic target in a rodent model of hemorrhagic shock: effect of different resuscitation strategies on lung and liver. *Surgery* 141:784–794.

Mabuchi A, Wake K, Marlini M, Watanabe H, and Wheatley AM (2009) Protection by glycyrrhizin against warm ischemia-reperfusion-induced cellular injury and

derangement of the microcirculatory blood flow in the rat liver. *Microcirculation* **16**:364–376.

Marwali MR and Mehta JL (2006) COX-2 inhibitors and cardiovascular risk. Inferences based on biology and clinical studies. *Thromb Haemost* **96**:401–406.

Mi Q, Constantine G, Ziraldo C, Solovyev A, Torres A, Namas R, Bentley T, Billiar TR, Zamora R, and Puyana JC, et al. (2011) A dynamic view of trauma/hemorrhage-induced inflammation in mice: principal drivers and networks. *PLoS ONE* **6**:e19424.

Mollen KP, Anand RJ, Tsung A, Prince JM, Levy RM, and Billiar TR (2006) Emerging paradigm: toll-like receptor 4-sentinel for the detection of tissue damage. *Shock* **26**:430–437.

Namas R, Ghuma A, Hermus L, Zamora R, Okonkwo DO, Billiar TR, and Vodovotz Y (2009) The acute inflammatory response in trauma / hemorrhage and traumatic brain injury: current state and emerging prospects. *Libyan J Med* **4**:97–103.

Newton K and Dixit VM (2012) Signaling in innate immunity and inflammation. *Cold Spring Harb Perspect Biol* **4**:1–19.

Ogiku M, Kono H, Hara M, Tsuchiya M, and Fujii H (2011) Glycyrrhizin prevents liver injury by inhibition of high-mobility group box 1 production by Kupffer cells after ischemia-reperfusion in rats. *J Pharmacol Exp Ther* **339**:93–98.

Parrish W and Ulloa L (2007) High-mobility group box-1 isoforms as potential therapeutic targets in sepsis. *Methods Mol Biol* **361**:145–162.

Peitzman AB, Billiar TR, Harbrecht BG, Kelly E, Udekwu AO, and Simmons RL (1995) Hemorrhagic shock. *Curr Probl Surg* **32**:925–1002.

Peltz ED, Moore EE, Eckels PC, Damle SS, Tsuruta Y, Johnson JL, Sauaia A, Silliman CC, Banerjee A, and Abraham E (2009) HMGB1 is markedly elevated within 6 hours of mechanical trauma in humans. *Shock* **32**:17–22.

Pergel A, Kanter M, Yucel AF, Aydin I, Erboga M, and Guzel A (2012) Anti-inflammatory and antioxidant effects of infliximab in a rat model of intestinal ischemia/reperfusion injury. *Toxicol Ind Health* **28**:923–932.

Rajnik M, Salkowski CA, Thomas KE, Li YY, Rollwagen FM, and Vogel SN (2002) Induction of early inflammatory gene expression in a murine model of non-resuscitated, fixed-volume hemorrhage. *Shock* **17**:322–328.

Reichel CA, Khandoga A, Anders HJ, Schlöndorff D, Luckow B, and Krombach F (2006) Chemokine receptors Ccr1, Ccr2, and Ccr5 mediate neutrophil migration to postischemic tissue. *J Leukoc Biol* **79**:114–122.

Roumen RM, Hendriks T, van der Ven-Jongekrijg J, Nieuwenhuijzen GA, Sauerwein RW, van der Meer JW, and Goris RJ (1993) Cytokine patterns in patients after major vascular surgery, hemorrhagic shock, and severe blunt trauma. Relation with subsequent adult respiratory distress syndrome and multiple organ failure. *Ann Surg* **218**:769–776.

Sakurai H, Suzuki S, Kawasaki N, Nakano H, Okazaki T, Chino A, Doi T, and Saiki I (2003) Tumor necrosis factor-alpha-induced IKK phosphorylation of NF-kappaB

p65 on serine 536 is mediated through the TRAF2, TRAF5, and TAK1 signaling pathway. *J Biol Chem* **278**:36916–36923.

Subramaniam D, May R, Sureban SM, Lee KB, George R, Kuppusamy P, Ramanujam RP, Hideg K, Dieckgraefe BK, and Houchen CW, et al. (2008) Diphenyl difluoroketone: a curcumin derivative with potent in vivo anticancer activity. *Cancer Res* **68**:1962–1969.

Takahashi T, Shimizu H, Morimatsu H, Inoue K, Akagi R, Morita K, and Sassa S (2007) Heme oxygenase-1: a fundamental guardian against oxidative tissue injuries in acute inflammation. *Mini Rev Med Chem* **7**:745–753.

Takahashi T, Shimizu H, Morimatsu H, Maeshima K, Inoue K, Akagi R, Matsumi M, Katayama H, and Morita K (2009) Heme Oxygenase-1 is an Essential Cytoprotective Component in Oxidative Tissue Injury Induced by Hemorrhagic Shock. *J Clin Biochem Nutr* **44**:28–40.

Takami S, Minami M, Nagata I, Namura S, and Satoh M (2001) Chemokine receptor antagonist peptide, viral MIP-II, protects the brain against focal cerebral ischemia in mice. *J Cereb Blood Flow Metab* **21**:1430–1435.

Tamion F, Richard V, Bonmarchand G, Leroy J, Lebreton JP, and Thuillez C (2001) Induction of heme-oxygenase-1 prevents the systemic responses to hemorrhagic shock. *Am J Respir Crit Care Med* **164**:1933–1938.

Tasdemir C, Tasdemir S, Vardi N, Ates B, Parlakpinar H, Kati B, Karaaslan MG, and Acet A (2012) Protective effect of infliximab on ischemia/reperfusion-induced damage in rat kidney. *Ren Fail* **34**:1144–1149.

Tell G, Damante G, Caldwell D, and Kelley MR (2005) The intracellular localization of APE1/Ref-1: more than a passive phenomenon? *Antioxid Redox Signal* **7**:367–384.

Tsatsanis C, Androulidaki A, Venihaki M, and Margioris AN (2006) Signalling networks regulating cyclooxygenase-2. *Int J Biochem Cell Biol* **38**:1654–1661.

van Berlo D, Knaapen AM, van Schooten FJ, Schins RP, and Albrecht C (2010) NF-kappaB dependent and independent mechanisms of quartz-induced proinflammatory activation of lung epithelial cells. *Part Fibre Toxicol* **7**:13–33.

Vilekar P, Awasthi S, Natarajan A, Anant S, and Awasthi V (2012) EF24 suppresses maturation and inflammatory response in dendritic cells. *Int Immunol* **24**:455–464.

Villavicencio RT and Billiar TR (1999) The role of nitric oxide in the initiation of inflammation in shock, in *Immune response in the Critically Ill* (Marshall JC, Cohen JC, and Vincent J-L, eds, ed) pp 182–189, Springer-Verlag, Berlin, Heidelberg.

Wu KK (2006) Transcription-based COX-2 inhibition: a therapeutic strategy. *Thromb Haemost* **96**:417–422.

Address correspondence to: Vibhudutta Awasthi, Department of Pharmaceutical Sciences, 1110 North Stonewall Avenue, Oklahoma City, OK 73117. E-mail: Vibhudutta-Awasthi@ouhsc.edu